

reorganization energy and an increase in the probability of forming the precursor complex with increasing size.

The maximum variation in rate with pressure is about a factor of 2 for 100 MPa. On the basis of the variation of rate with the estimated radii previously observed at 1 atm for these complexes,⁷ the variation with pressure could be explained by a change in electron-transfer distance of about 0.1 Å for a pressure change of 100 MPa. The trend in ΔV^\ddagger appears to be related to the flexibility of the ligands more than any other parameter. The more flexible ligands, those that can form a smaller complex by a change in conformation, give the more negative ΔV^\ddagger values. These changes in volume of the reactants through changes in ligand conformation are part of the intrinsic volume component and can be understood as follows. Assuming that electron transfer is especially sensitive to the Mn-Mn distance, the transition state will have the ligands between the Mn centers in their most compact conformations at a given pressure. The reactants must assume this more compact conformation before collision to form the precursor complex takes place. Thus there is formally a conformational preequilibrium between the ground state and the compact state, with a negative ΔV . The complexes with inflexible ligands will not show this effect and will give more positive values of ΔV^\ddagger . The contribution from the electrostatic component is not zero, but is probably constant within $\pm 3 \text{ cm}^3/\text{mol}$ as in the estimates made of it.

It has been previously observed that curvature of the $\ln k$ vs. P plots, apparent $\Delta\beta^\ddagger$ different from zero, is associated with changes in solvation.³³ This could be the case for the *n*-butyl isocyanide complexes, but it is not clear why only these ions should show this effect, when other ones, such as the ethyl isocyanide complexes, are at least as solvent accessible. Another interpretation, consistent with the proportionality between ΔV^\ddagger and $\Delta\beta^\ddagger$, is that the ligand flexibility decreases with pressure, and thus $\Delta\beta^\ddagger$

is negative and proportional to ligand flexibility and ΔV^\ddagger . It is reasonable to expect ligand flexibility to decrease with pressure since as the ligand adopts a more compact conformation, its ability to compact further merely through conformational changes is decreased.

The other activation parameters can now be considered. These have been discussed previously in more detail.^{7,8} To summarize, the observation is that the rate variation with ligand is entirely the result of a change in enthalpy. The simplest interpretation of this is that the larger complexes must distort to allow the manganese centers to approach to a comparable electron-transfer distance regardless of ligand. This is consistent with the negative volumes of activation arising from reaction through a compact form of the complex. It is also possible that the variation of electron-transfer rate with ligand at ambient pressure is due wholly or partly to a change in electron-transfer distance. If this is the case, the entropies of activation should have become less favorable with decreasing rate, and there should not have been a significant difference in intrinsic volume between the transition state and the reactants. It is likely that both electron-transfer distance and selective reactivity of intrinsically smaller ions is involved, along with solvent effects that cause compensation between the activation parameters. These questions are important ones if any understanding of the effect of the medium on electron-transfer reactivity is to be attained. Better models for the precursor association and solvent reorganization properties are needed, as are further results on rate constants and activation parameters as a function of solvent. Data on the molal volumes of large ions of different charges in organic solvents at concentrations typical for kinetic measurements would help greatly in the second method used to estimate ΔV^\ddagger . The work presented here is being extended through a study of the volume of activation as a function of solvent and ionic strength.

Acknowledgment. The authors wish to acknowledge the assistance of Don Appel with the measurements on the Nicolet NMR instrument. This work was supported by the National Science Foundation and by the Boeing Co. through funds for the purchase of the Nicolet instrument.

Supplementary Material Available: Tables of reactant concentrations, temperatures, and line widths (5 pages). Ordering information is given on any current masthead page.

- (29) Brown, B. M.; Sutin, N. *J. Am. Chem. Soc.* **1979**, *101*, 883.
 (30) Yang, E. S.; Chan, M.-S.; Wahl, A. C. *J. Phys. Chem.* **1980**, *84*, 3094.
 (31) Beattie, J. K.; Binstead, R. A.; Broccardo, M. *Inorg. Chem.* **1978**, *17*, 1822.
 (32) Szecsy, A. P.; Haim, A. *J. Am. Chem. Soc.* **1981**, *103*, 1679.
 (33) Swaddle, T. W. In *High Pressure Science and Technology*; Timmerhaus, K. D., Barber, M. S., Eds.; Plenum: New York; 1979; Vol. 1, p 631.

Contribution from the Department of Chemistry and the Biochemistry Program, The Pennsylvania State University, University Park, Pennsylvania 16802

Stopped-Flow Study of Ligand-Exchange Kinetics between Terbium(III) Ion and Calcium(II) Ethylenediaminetetraacetate

Patrick J. Breen, William DeW. Horrocks, Jr.,* and Kenneth A. Johnson

Received January 15, 1985

Exchange of EDTA between calcium(II) and terbium(III) in the pH range 4.4-6.0 was studied by using a stopped-flow spectrophotometer to monitor the increase in Tb^{3+} luminescence as it binds EDTA. The data suggest competing pathways for exchange of the ligand in the pH range 5.0-6.0, involving either a direct attack by Tb^{3+} followed by release of Ca^{2+} or a faster, H^+ -catalyzed process involving the dissociation of $\text{CaH}(\text{EDTA})^-$ followed by rapid binding of Tb^{3+} . Evidence for an additional pathway of dissociation of $\text{Ca}(\text{EDTA})^{2-}$ at pH values less than 5.0 is also presented.

Introduction

The substitution of tripositive lanthanide ions, Ln^{3+} , for Ca^{2+} in biomolecular systems has been shown to be a useful technique for probing such systems.^{1,2} A logical step toward understanding the binding of these ions to macromolecules is first to characterize the kinetics of binding to model systems such as polycarboxylate

ligands, e.g. EDTA, which are potential models for the calcium-binding sites in proteins. We focus our attention on EDTA as the ligand in this study because the rate of exchange of EDTA between Ca^{2+} and Tb^{3+} occurs on a time scale which can be conveniently measured on a stopped-flow spectrophotometer.

A large volume of work exists concerning the kinetics of exchange between chelated and unchelated metal ions of various types including the lanthanides and actinides.³⁻²⁷ Most studies

- (1) Horrocks, W. D., Jr.; Sudnick, D. R. *Science (Washington, D.C.)* **1979**, *206*, 1194-1196.
 (2) Horrocks, W. D., Jr.; Sudnick, D. R. *Acc. Chem. Res.* **1981**, *14*, 384-392.

- (3) D'Olieslager, W.; Oeyen, A. *J. Inorg. Nucl. Chem.* **1978**, *40*, 1565-1570.

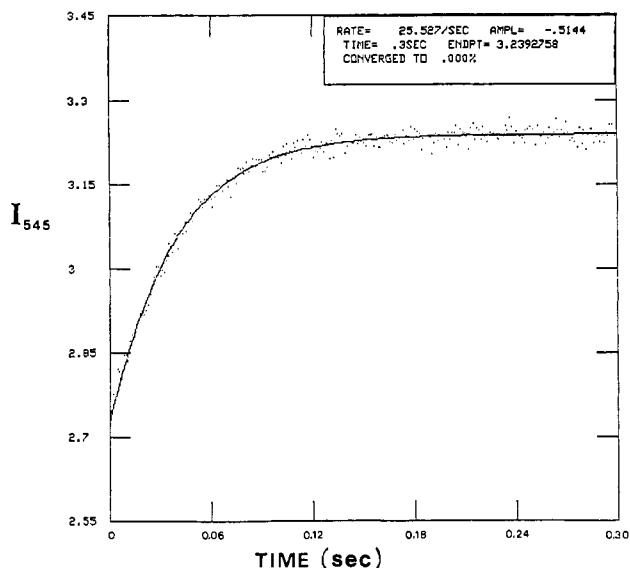


Figure 1. Kinetic trace of Tb(III) luminescence as a function of time (0.10 M $TbCl_3$ mixed with 0.02 M EDTA and 0.02 M $CaCl_2$, pH 5.6).

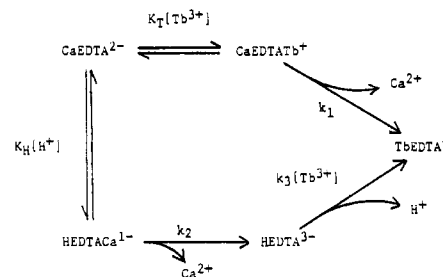
involving lanthanide ions have employed radiotracer methods to study the isotope-exchange reactions of these metal ions bound to polyaminopolycarboxylate ligands. It is generally believed that dissociation of lanthanide ions from EDTA and other polyamino polycarboxylates follows a two-path mechanism, with one path involving protonation and dissociation of the complex and the other path being an acid-independent dissociation. Several studies have provided evidence for the formation of bridged binuclear intermediates in the acid-independent dissociation step.^{5,6,10-12} This work also provides evidence for the existence of such an intermediate.

One of the objectives of this study was to assess the utility of Tb^{3+} luminescence to study the exchange of Ca^{2+} and this ion in EDTA complexes by using a stopped-flow spectrophotometer. An understanding of the mechanism of metal, ion dissociation from polyamino polycarboxylates is potentially helpful in understanding metal ion dissociation from proteins, since calcium-binding sites

Table I. Slopes and y -Intercepts as a Function of pH Calculated from Least-Squares Fits of Figure 2

pH	slope	y -intercept	pH	slope	y -intercept
4.4	16.7 ± 2.1	11.9 ± 15.9	5.6	0.29 ± 0.09	16.9 ± 1.3
4.8	3.65 ± 0.5	19.4 ± 4.6	6.0	0.10 ± 0.02	15.7 ± 0.6
5.0	1.14 ± 0.1	20.7 ± 2.2			17.36 (av)
5.2	0.58 ± 0.12	19.0 ± 1.9			

Scheme I



in proteins typically involve several carboxylate moieties.

The luminescence of Tb^{3+} increases when a ligand binds to it due to the displacement of coordinated water molecules. The O-H vibrational manifold of coordinated water provides a nonradiative pathway for deexcitation of Tb^{3+} , thereby reducing its lifetime and quantum yield. The kinetic data of the present study were obtained by monitoring the increase in Tb^{3+} luminescence produced as it is sequestered by EDTA, replacing Ca^{2+} .

Experimental Section

Kinetic traces were obtained with a stopped-flow spectrophotometer described elsewhere.²⁸ Excitation of the Tb^{3+} was achieved with a band-pass filter in the wavelength range of 360–400 nm while the relatively intense Tb^{3+} emission was monitored at 545 nm with a narrow-band-pass filter (6-nm half-bandwidth) at right angles to the exciting beam. All measurements were made at 25 °C on solutions prepared from doubly distilled, deionized water.

A solution, equimolar in EDTA and $CaCl_2$, was placed in one stopped-flow syringe, and a solution of $TbCl_3$ at least five times as concentrated was placed in the other syringe. Tb^{3+} binds EDTA approximately 10^8 times more strongly than Ca^{2+} ($K_A^{Tb} \approx 10^{18} M^{-1}$ vs. $K_A^{Ca} \approx 10^{10} M^{-1}$)^{18,29} so that the exchange reaction is essentially irreversible. Kinetic measurements were carried out at pH values of 6.0, 5.6, 5.2, 4.8, and 4.4. The data were fit to a single exponential by using a method of moments exponential analysis. Solutions at pH 5.0, 4.8, and 4.4 were buffered with 0.1 M 3,5-dichloropyrazole. Solutions at pH 6.0 and 5.6 were buffered with 0.1 M piperazine. At pH 5.2, 0.1 M hexamethylenetetramine was used. These buffers were chosen because they bind lanthanide ions very poorly and thus do not interfere in the reaction of Tb^{3+} with calcium-bound EDTA. Acetate buffer has been used in the past by most other authors; however, this ion has been shown to affect the rates of metal ion dissociation,^{4,11,14,20} and thus complicate the kinetics. It was not used in this study.

Results

Figure 1 shows a typical kinetic trace obtained in the course of this work. As can be seen, the signal-to-noise ratio is good, allowing accurate determination of the rate constants.

Figure 2 is a plot of the observed rate constant, λ , vs. the reciprocal of the Tb^{3+} concentration for each pH, with the best fit least-squares line drawn through each set of points. The linear fits for all six data sets extrapolate to approximately the same y -intercept value. Table I lists the slopes and y -intercepts obtained from the least-squares fits of Figure 2. These data reveal the startling fact that as the concentration of the competing Tb^{3+} ion increases, the rate of its substitution for Ca^{2+} in EDTA actually decreases. This effect becomes more pronounced as the pH decreases. Such a trend has not been previously reported.

A model that accounts for the observed data and that has features in common with one used⁶ to interpret the exchange of

- (4) Choppin, G. R.; Williams, K. R. *J. Inorg. Nucl. Chem.* **1973**, *35*, 4255–4269.
- (5) Brücher, E.; Laurency, G. *J. Inorg. Nucl. Chem.* **1981**, *43*, 2089–2096.
- (6) Brücher, E.; Laurency, G. *Inorg. Chem.* **1983**, *22*, 338–342.
- (7) D'Olieslager, W.; Choppin, G. R. *J. Inorg. Nucl. Chem.* **1971**, *33*, 127–135.
- (8) Balcombe, C. I.; Wiseall, B. *J. Inorg. Nucl. Chem.* **1973**, *35*, 2859–2869.
- (9) Brücher, E.; Szarvas, P. *Inorg. Chim. Acta* **1970**, *4*, 632–636.
- (10) Williams, K. R.; Choppin, G. R. *J. Inorg. Nucl. Chem.* **1974**, *36*, 1849–1853.
- (11) Glentworth, P.; Wiseall, B.; Wright, C. L.; Mahmood, A. J. *J. Inorg. Nucl. Chem.* **1968**, *30*, 967–986.
- (12) Asano, T.; Okada, S.; Sakamoto, K.; Taniguchi, S.; Kobayashi, Y. *J. Inorg. Nucl. Chem.* **1969**, *31*, 2127–2133.
- (13) Glentworth, P.; Newton, D. A. *J. Inorg. Nucl. Chem.* **1971**, *33*, 1701–1715.
- (14) Ryhl, T. *Acta Chem. Scand.* **1972**, *26*, 3955–3968.
- (15) Ryhl, T. *Acta Chem. Scand.* **1973**, *27*, 303–314.
- (16) Margerum, D. W. *Rec. Chem. Prog.* **1963**, *24*, 237–251.
- (17) Margerum, D. W.; Janes, D. L.; Rosen, H. M. *J. Am. Chem. Soc.* **1965**, *87*, 4463–4472.
- (18) Kula, R. J.; Reed, G. H. *Anal. Chem.* **1966**, *38*, 697–701.
- (19) Kuempel, J. R.; Schaap, W. *Inorg. Chem.* **1968**, *7*, 2435–2442.
- (20) Balcombe, C. I.; Wiseall, B. *J. Inorg. Nucl. Chem.* **1974**, *36*, 881–885.
- (21) Kim, I. H.; Yan, S. S. *Polyhedron* **1982**, *1*, 707–709.
- (22) Brücher, E.; Bányai, I.; Krusper, L. *Acta Chim. Hung.* **1984**, *115*, 39–50.
- (23) Nyssen, G. A.; Margerum, D. W. *Inorg. Chem.* **1970**, *9*, 1814–1820.
- (24) Bydalek, T. J.; Margerum, W. D. *J. Am. Chem. Soc.* **1961**, *83*, 4326–4329.
- (25) Margerum, D. W.; Zabin, B. A.; Janes, D. L. *Inorg. Chem.* **1966**, *5*, 250–255.
- (26) Margerum, D. W. *J. Phys. Chem.* **1959**, *63*, 336–339.
- (27) Margerum, D. W.; Byalek, T. J. *Inorg. Chem.* **1962**, *1*, 852–856.

- (28) Johnson, K. A.; Porter, M. E. *J. Biol. Chem.* **1983**, *258*, 6582–6587.
- (29) Schwarzenbach, G.; Gut, R.; Anderegg, G. *Helv. Chim. Acta* **1954**, *37*, 937–942.

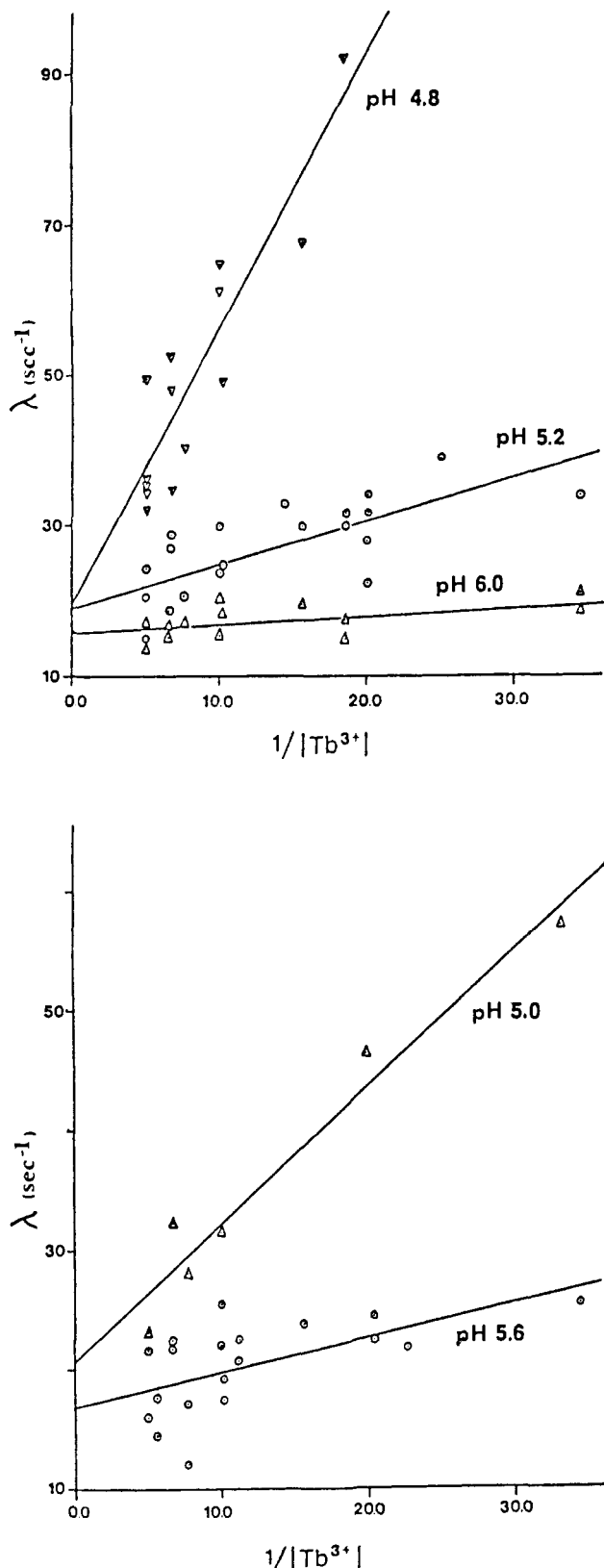


Figure 2. Observed rate constant, λ , as a function of inverse Tb^{3+} concentration at a variety of pHs, with best-fit least-squares lines drawn.

Pb^{2+} , Co^{2+} , and Ni^{2+} ions with Ce^{3+} in $Ce(EDTA)^-$ is given in Scheme I.

While it has been proposed^{7,11,12} that the protonation of EDTA complexes is a slow step, followed by rapid dissociation, Ryhl^{14,15} has presented ¹H NMR spectral data which led him to conclude that such protonation is in fact a rapid process, with cleavage of the metal-nitrogen bond being the rate-determining step of the dissociation. For this reason, it is assumed that the equilibrium

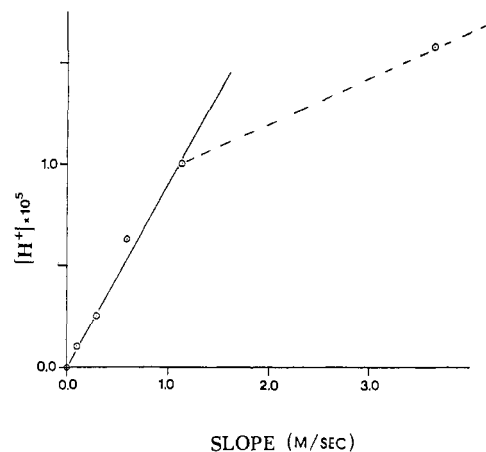


Figure 3. Slope of the line at each pH from Figure 2 vs. $[H^+]$ (pH 4.4 point not shown).

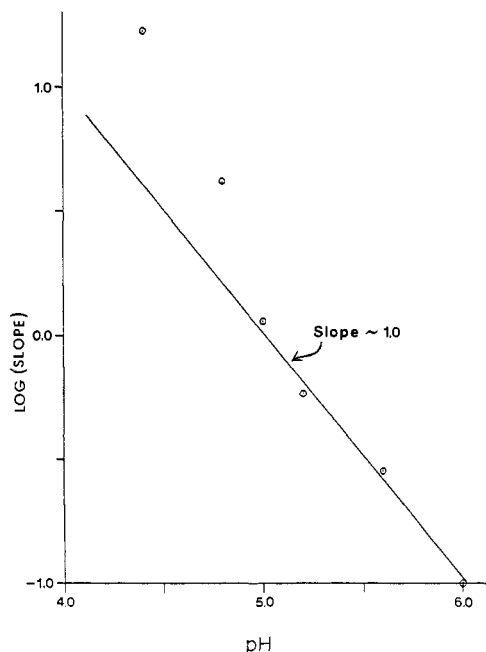


Figure 4. Plot of $[H^+]$ vs. $\log(\text{slope})$ illustrating the good fit to a line of unit slope of data above pH 5.0.

between $Ca(EDTA)^{2-}$ and $CaH(EDTA)^-$ is a fast equilibrium.

If one assumes K_T and K_H to denote rapid equilibria and k_1 and k_2 relatively slow rate processes, the overall rate constant, λ , for the appearance of $Tb(EDTA)^-$ will be given by

$$\lambda = \frac{k_1 K_T [Tb^{3+}] + k_2 K_H [H^+]}{1 + K_H [H^+] + K_T [Tb^{3+}]} \quad (1)$$

The derivation of this expression is presented in the Appendix.

Since $K_T [Tb^{3+}] \gg 1$, $K_H [H^+]$, eq 1 reduces to

$$\lambda = k_1 + \frac{k_2 K_H [H^+]}{K_T} \frac{1}{[Tb^{3+}]} \quad (2)$$

which fits the trend observed in Figure 2.

From eq 2 it can be seen that a plot of λ vs. $1/[Tb^{3+}]$ should have k_1 as the y -intercept and $k_2 K_H [H^+]/K_T$ as the slope. k_1 was calculated from Figure 2 to be $\sim 18 \text{ s}^{-1}$.

A plot of the individual slopes from Figure 2 vs. pH should also be a straight line passing through the origin with a slope equal to $k_2 K_H / K_T$ (Figure 3). In Figure 3 the points for pH 4.8 and 4.4 deviate significantly from the predicted line. Kula and Reed¹⁸ calculated the concentrations of various species in a 1:1 solution of Ca^{2+} and EDTA as a function of pH. At pH values less than 5.0, significant amounts of H_2EDTA^{2-} and $CaH(EDTA)^-$ are present in solution. It is likely that, under these low-pH conditions,

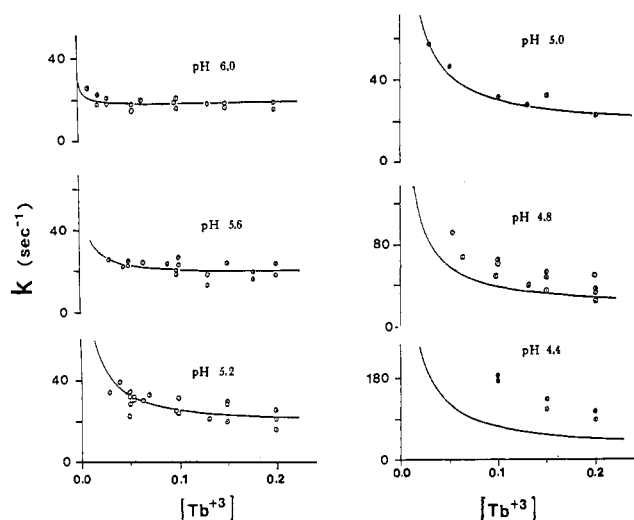


Figure 5. Composite figure showing the fit of the observed data to curves calculated from the theoretical model proposed, using the rate and equilibrium constants noted in the text.

an additional pathway contributes significantly to the overall observed rate by increasing the amounts of $\text{H}_2\text{EDTA}^{2-}$ and $\text{CaH}(\text{EDTA})^-$ in solution.

The slope of the line through the points taken at pH values above 5.0 in Figure 3 is approximately 10^5 . From this it follows that

$$\frac{k_2 K_H}{K_T} = 10^5 \text{ s}^{-1}$$

Kula and Reed¹⁸ report values of $K_H \approx 650 \text{ M}^{-1}$ and $k_2 = 5 \times 10^4 \text{ s}^{-1}$. Substitution of these numbers into the above expression yields a K_T value of 325 M^{-1} . Values of $K_H = 1000 \text{ M}^{-1}$ and $k_2 = 3 \times 10^4 \text{ s}^{-1}$, which are close to the literature values, yield a value of 200 M^{-1} for K_T . Theoretical curves calculated from these numbers fit the observed data quite well (Figure 5) at pH values greater than or equal to 5.0. The lack of agreement at pH values less than 5.0 is likely due to the increased amounts of $\text{H}_2\text{EDTA}^{2-}$ and $\text{CaH}(\text{EDTA})^-$, as discussed previously.

Discussion

The model presented is able to account well for the two major trends observed in the data, namely, a strong dependence of the observed rate constant on pH and the rate-reducing effect of increasing Tb^{3+} concentration. These two trends are clearly correlated, since the dependence of the rate constant on Tb^{3+} concentration becomes less and less pronounced as the pH is increased. This would be expected if there were two competing pathways, i.e., a fast attack by Tb^{3+} to form a bridged intermediate, with a relatively slow dissociation of Ca^{2+} to yield $\text{Tb}(\text{EDTA})^-$, vs. a fast H^+ -catalyzed dissociation of $\text{Ca}(\text{EDTA})^{2-}$ followed by fast binding of the free ligand to Tb^{3+} to form $\text{Tb}(\text{EDTA})^-$.

The postulation of an extra pathway of dissociation of $\text{Ca}(\text{EDTA})^{2-}$ at pH values less than 5.0 is reasonable in light of the calculations done by Kula and Reed¹⁸ which show that below pH 5.0 significant quantities of $\text{H}_2\text{EDTA}^{2-}$ exist in a 1:1 solution of EDTA and Ca^{2+} and the findings of others that a $[\text{H}^+]^2$ term appears in the rate expression for the exchange of Ln^{3+} ions in polycarboxylate complexes.^{8,9,11-14}

The kinetic mechanism outlined in Scheme I suggests that there should be an initial increase in luminescence observed as Tb^{3+} forms the mixed-metal EDTA intermediate. This initial increase was not observed in the kinetic traces since this initial step occurs within the mixing time of the stopped-flow instrument. The trace obtained reflects only the increase in luminescence resulting from the final dissociation of Ca^{2+} (k_1) to yield $\text{Tb}(\text{EDTA})^-$.

The presently proposed mechanism suggests that dissociation of protonated $\text{Ca}(\text{EDTA})^{2-}$ ($\text{CaH}(\text{EDTA})^-$) is much more rapid than the dissociation of Ca^{2+} from an intermediate binuclear $\text{CaTb}(\text{EDTA})^+$ complex. Why this is the case is not clear, al-

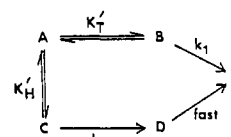
though such behavior has been reported in several EDTA/transition-metal studies.^{16,17,19}

The technique of using the increased Tb^{3+} luminescence exhibited by Tb^{3+} upon binding a ligand has been shown to be useful in following the kinetics of binding. Analogous techniques have recently been employed by us to study the kinetics of exchange or removal of metal ions in metal-binding proteins.³⁰

Acknowledgment. This research was supported by the National Science Foundation through Grant CHE82-05127.

Appendix. Derivation of Eq 1 from Scheme I

The reaction sequence outlined in Scheme I may be more simply illustrated as



where $K'_T = K_T[\text{Tb}^{3+}]$ and $K'_H = K_H[\text{H}^+]$. Since a rapid equilibrium exists between A and B and between A and C

$$[\text{B}] = K'_T[\text{A}] \quad (\text{A1})$$

and

$$[\text{C}] = K'_H[\text{A}] \quad (\text{A2})$$

The time dependency of [E] can be written

$$[\dot{\text{E}}] = k_1[\text{B}] + k_2[\text{C}]$$

or

$$[\dot{\text{E}}] = k_1 K'_T[\text{A}] + k_2 K'_H[\text{A}] = (k_1 K'_T + k_2 K'_H)[\text{A}] \quad (\text{A3})$$

If the total concentration of A, B, C, and E is normalized to 1

$$[\text{A}] + [\text{B}] + [\text{C}] + [\text{E}] = 1$$

then

$$[\text{A}] + [\text{B}] + [\text{C}] = 1 - [\text{E}]$$

and by substitution of eq A1 and A2

$$[\text{A}] + K'_T[\text{A}] + K'_H[\text{A}] = 1 - [\text{E}]$$

which can be written as

$$[\text{A}] = \frac{1 - [\text{E}]}{1 + K'_H + K'_T}$$

This expression can be substituted into eq A3 to give

$$[\dot{\text{E}}] = \frac{(k_1 K'_T + k_2 K'_H)(1 - [\text{E}])}{1 + K'_H + K'_T}$$

which can be rearranged to give the differential equation describing the time dependence of [E], in an easily solvable form:

$$[\dot{\text{E}}] = \left(\frac{k_1 K'_T + k_2 K'_H}{1 + K'_H + K'_T} \right) [\text{E}] - \frac{k_1 K'_T + k_2 K'_H}{1 + K'_H + K'_T}$$

The solution for this equation is of the form

$$[\text{E}] = \alpha_0 + \alpha_1 e^{-\lambda_1 t}$$

where

$$\lambda_1 = \frac{k_1 K'_T + k_2 K'_H}{1 + K'_H + K'_T} = \frac{k'_1 K_T[\text{Tb}^{3+}] + k'_2 K_H[\text{H}^+]}{1 + K_H[\text{H}^+] + K_T[\text{Tb}^{3+}]}$$

This is eq 1. α_0 and α_1 are determined from boundary conditions on [E]:

$$\text{at } t = 0, \quad [\text{E}] = 0 = \alpha_0 + \alpha_1$$

$$\text{at } t = \infty, \quad [\text{E}] = 1 = \alpha_0$$

yielding the final expression for [E]

$$[\text{E}] = 1 - e^{-\lambda_1 t}$$